Bond Graph based Multiphysic Modelling of Anion Exchange Membrane Water Electrolysis Cell*

Sumit Sood[1]; Belkacem Ould Bouamama[1]; Jean-Yves Dieulot[1]; Mathieu Bressel[2]; Xiaohong Li[3]; Habib Ullah[3] and Adeline Loh[3]

***Abstract*— This work is an attempt to develop and validate a graphical dynamical model of an AEM electrolysis cell based on Bond Graphs, an energy based tool that allows to represent multiphysics systems. The model of the cell lays a foundation for developing a complete representation for AEM electrolysers which can be used for simulation as well as for developing control algorithms and fault diagnosis. Parameter identification and model validation is achieved using experimental data.**

I. INTRODUCTION

Hydrogen has emerged as a carbon neutral way of storing surplus electricity available from renewable energy resources at off peak hours due to its intermittent nature. Hydrogen is in abundance (can be produced from water), can be stored with ease and is the clean and lightest fuel with highest energy density[1]. Hydrogen production through water electrolysis is the most matured technology and can be easily coupled with any source of electricity[2].

Electrolysis is the technique through which the water molecules are split into hydrogen and oxygen gases under the influence of the electric current[3]. Two types of electrolysis techniques, namely alkaline electrolysis and proton exchange membrane (PEM) electrolysis are well developed and highly used on the commercial scale[4]. These two techniques have numerous advantages and disadvantages which are shown in Table I.

In the recent years, in order to benefit from the advantages of both alkaline and PEM electrolysis polymer based Anion Exchange Membranes (AEM) have been developed. PEM electrolyser uses noble earth metals such as Ir, Ru, and Pt etc., which are expensive and limit its commercial applications. On the other hand, AEM electrolyser is based on alkaline electrolytes so, a wide range of earth-abundant transition metals and their oxides can be employed [5]. These membranes have made their way to the fuel cells but it is still under development for electrolysis [4]. To adapt AEM as a reliable technology for water electrolysis significant improvements are required[4]. Research is being carried out in order to achieve desirable properties for the membrane such as better mechanical stability, ionic conductivity, longer life, lower cost etc. To finally assemble this into a functional and efficient electrolyser is yet another challenge.

Modelling and simulation are very powerful tools of modern engineering that can also contribute towards these goals by providing alternate means for design investigation and operating conditions optimization by spending less time and at relatively lower cost as compared to the physical experiments[6]. The importance of modelling and simulation increases many folds in case of dynamic multi-physics systems. AEM electrolysis cell is one such case in which complicated physio-chemical processes takes place. Modelling plays a significant role in quantifying such processes [7]. Models once developed can also be used for understanding the phenomenon, developing control for the system as well as for online Fault Detection and Isolation (FDI) to insure the safety of the personnel and the equipment. Numerous modelling techniques have been developed by the researchers that can be broadly classified under two categories, namely equation based and graphical based modelling.

In equation based modelling techniques, the system is represented in terms of ordinary or partial differential equations. These techniques are less user friendly and difficult to modify or update as the dynamic equations of the whole system are needed beforehand[8]. Distributed parameters dynamic models represented by Partial Differential Equations (PDE are also used for deep analysis, but this kind of models are not suited for control and diagnosis tasks. The models (complex and resolved using finite elements) are used mainly for sizing, chemical and thermal process design and analysis[9]. In graphical based modelling approaches, the model of the system is represented by connecting the graphical models of subsystems (known as blocks) through ports based on their physical interactions. It is easy to understand the physical structure as well as the behaviour of the system through such models. These approaches are more user friendly and physical phenomenon are clearly displayed.

Many graphical modelling techniques are available out of which bond graph is of significant interest. Bond graph is based on power exchange between the components of the system and is domain independent which makes it well suited for multi-physics systems. This unified tool can represent four different levels of modelling [6]:technological (architectural model given by by word bond graph), physical (to display different physical phenomena by bond graph

*This work is funded under Interreg 2seas E2C project (subsidiary contract nr. 2S03-019)

[1]Sumit Sood, Belkacem Ould Bouamama and Jean-Yves Dieulot are with CRISTAL UMR CNRS 9189, Université de Lille, Villeneuve d'Ascq, France. sumit.sood@univ-lille.fr; belkacem.ouldbouamama@polytech-lille.fr; jean-yves.dieulot@univ-lille.fr

[2]Mathieu Bressel is with CRISTAL UMR CNRS 9189, Yncréa , Villeneuve d'Ascq, France. mathieu.bressel@yncrea.fr

[3]MXiaohong Li; Habib Ullah and Adeline Loh are with Renewable Energy Group, College of Engineering Mathematics and Physical Sciences, Cornwall, UK. X.Li@exeter.ac.uk; hu203@exeter.ac.uk; adeline.loh@exeter.ac.uk

TABLE I

ADVANTAGES AND DISADVANTAGES OF ALKALINE, PEM AND AEM ELECTROLYSIS[4]

Alkaline	PEM	AEM
	Advantages	
Mature technology	Higher performance	Non-noble metal catalyst
Non-PGM catalyst	Higher voltage efficiency	Non-corrosive electrolyte
Long term stability	Good partial load	Compact cell design
Low cost	Rapid system response	Low cost
Megawatt range	Compact cell design	Absence of leaking
Cost effective	Dynamic operation	High operating pressure
	Disadvantages	
Low current densities	High cost of components	Laboratory stage
Crossover of gas	Acidic corrosive components	Low current densities
Low dynamic	Possible low durability	Durability
Low operating pressure	Noble metal catalyst	Membrane degradation
Corrosive liquid electrolyte	Stack below Megawatt range	Excessive catalyst loading

element), mathematical (dynamic equation are systematically deduced from the bond graph) and algorithmic level (by causalities assignment to generate simulation block diagram). Another key advantage of using bond graph is that the same model can be used for simulation as well as for control, sizing, diagnosis and prognosis.

Due to the maturity of the alkaline and PEM electrolysis techniques a lot of research has been done on the modelling of these type of electrolysers. A review proposed by Olivier et al. [2] exposed the existing models for the alkaline and low temperature PEM electrolysers. It shows that majority of the models are equation based (empirical or analytical) and are focused on understanding phenomena (including degradation mechanisms), characterization of performance, development of control for the system,diagnostic and prognostic (long-term durability evaluations). A very few graphical models exist for PEM electrolysers. Agbli et al. [10] proposed a graphical model based on energetic macroscopic representation (EMR) that can simulate the evolution of the temperature and included electro-chemical, electrical and thermal phenomena. They neglected the fluidic phenomenon. Zhou et al. [11] proposed a causal ordering graph (COG) based model to develop control algorithms for real time implementation in order to control power flow and hydrogen flow in a hybrid system containing electrolyser. A bond graph model proposed by Olivier et al. [6] for an industrial scale PEM electrolyser includes the auxiliaries of the electrolyser (Balance of plant). Different phenomenon like electro-chemical, thermal, fluidic, mass transfer have been incorporated into single model in order to study the effect on the overall performance of the model.

As AEM electrolysis is a new technique and is still being developed, there is not much work done on the modelling of such systems. There is only one mathematical model proposed by L. An et al. [7] that incorporates mass transport, charge transport and electro-chemical reaction in order to predict the performance of AEM electrolyser running on pure water. The model was validated by the experimental data available in the literature[12].

The lack of availability of a good model for AEM electrolyser warrants for the research in this area. The configuration of AEM electrolysis cell is similar to that of PEM [13]. There are some distinct differences such as the feed side, core chemical reactions etc. Because of this, models already developed for PEM can be modified and can be incorporated for AEM. The work presented in this paper is an attempt to take a step towards achieving this objective. Furthermore, this model can be used later for diagnosis and prognosis using structural and causal properties of the bond graph model. A dynamic multi-physic model based on bond graph theory has been developed for AEM electrolyser cell. The basic working principle of AEM electrolysis and the bond graph based modelling for AEM has been explained in section II. Once the bond graph model is generated, MATLAB Simulink model is systematically constructed through it for the simulations. Parameter identification and model validation are performed using experimental data from actual AEM cell. The methodology used is briefed in section III. The simulations performed and results obtained are presented in section IV.

II. BOND GRAPH MODELLING OF AEM

A. AEM Water Electrolysis

Schematic of an AEM water electrolysis cell is shown in Fig.1. The electrolyte is fed to the cell from the cathode

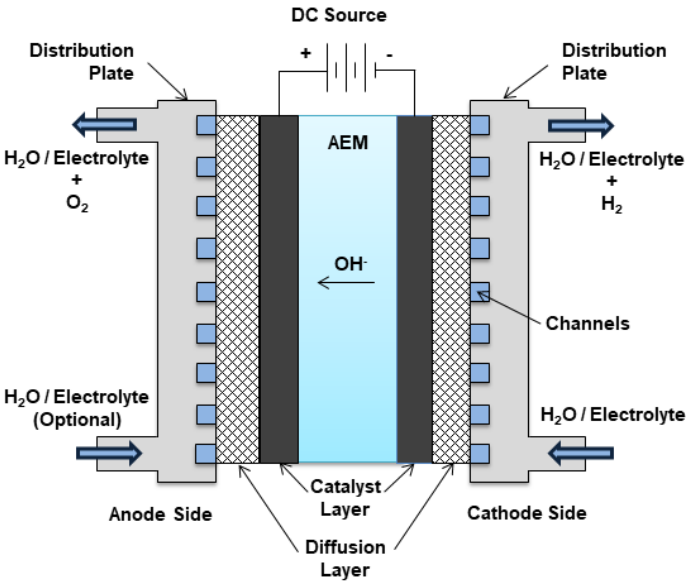

Fig. 1. Schematics of anion exchange membrane (AEM) water electrolysis

side where the water is reduced into hydrogen and hydroxyl ions are formed. These negative ions transport through the membrane towards the anode where they recombine to release oxygen. The electrolyte acts as a reagent as well as it facilitates the removal of the hydrogen at cathode. The electrolyte or water can also be fed to the anode side to facilitate the removal of oxygen depending on the design of

TABLE II

POWER VARIABLES FOR DIFFERENT ENERGY DOMAINS[6]

Physical Domain	Effort (e)	Flow (f)
Electrical	Voltage (V)	Current intensity (A)
Fluidic	Pressure (Pa)	Volume flow rate ($m^3 s^{-1}$)
Fluidic (Pseudo bond graph)	Pressure (Pa)	Mass flow ($kg\ s^{-1}$)
Thermal	Temperature (K)	Entropy flow ($JK^{-1}s^{-1}$)
Thermal (Pseudo bond graph)	Temperature (K)	Thermal flow (Js^{-1})
Chemical (Transformation)	Chemical Potential ($Jmol^{-1}$)	Molar flow ($mol\ s^{-1}$)
Chemical (Kinetic)	Chemical affinity ($Jmol^{-1}$)	Reaction speed flow rate ($mol\ s^{-1}$)

the cell. The half reactions on each electrode and overall reaction is given as [4]:

$$Anode: 4OH^- \rightarrow O_2 + 2H_2O + 4e^- \quad E_0 = 0.41\,V \tag{1}$$

$$Cathode: 4H_2O + 4e^- \rightarrow 2H_2 + 4OH^- \quad E_0 = -0.828\,V \tag{2}$$

$$Overall: H_2O(l) \rightarrow H_2(g) + \frac{1}{2}O_2(g) \quad E_0 = 1.23\,V \tag{3}$$

B. Bond Graph Modelling basics for multi-physics systems

Bond graph is a structure based modelling technique in which a system can be represented by predefined standard elements and junctions which in turn represent some physical phenomena. These elements are connected using the connectors known as power bonds that represent the power flow in the system. The bond graph is a unified approach as the elements are analogues irrespective of the physical domain to which the system belongs. The currency of interaction between the elements is power which is common to all the domains. This power exchange is labelled by two conjugated power variables named effort (e) and flow (f). However, the domains like chemical engineering can also be represented using this technique although the product of power variables is not power. Such models are known as pseudo bond graphs [6]. As shown in Fig. 2(a), the power exchanged between two systems A and B is indicated by a bond and half arrow represents the direction of power flow. One key structural property of the bond graph is the concept of causality. In the bond graph, it is represented by a cross-stroke on indicating the direction of the effort. This means that system A imposes effort on B and B impose flow in return on A as shown by the block diagram in Fig. 2 (b). Table II represents the power variables for some energy domains.

Fig. 2. Bond Graph representation (a) and relative block diagram (b) [14]

In bond graph almost all systems can be represented using hand full elements. These elements can be represented as a set:S=$\{R \cup C \cup I \cup TF \cup GY \cup SE \cup SF \cup De \cup Df \cup J\}$ [14]. Here R element represents energy dissipation. I and C elements represent the storage of kinetic and potential energy respectively.TF and GY are transformer and gyrator that represents the transformation of energy from one form to another. Se represents the source of effort and Sf represents the source of flow. De and Df are effort and flow sensors. J is junction which is used to connect the elements based on common effort (represented by 0) and common flow (represented by 1). it represents the law of conservation of energy. A multi-port RS element is also used for representing the resistance that also act like source. For example, a heating coil acts as a resistance for electricity bur also act as a source of thermal energy.

C. AEM Cell Bond Graph Modelling

AEM electrolysis cell is a multi-physics open system in which the physical inputs are electric current and electrolyte and the output is the hydrogen and oxygen gases. The modelling of such systems is not a trivial task and hence to simplify the modelling problem in hand following assumptions have been considered:

- The AEM cell operates under steady state conditions.
- The effect of diffusion is negligible on the cell voltage.
- The thermal capacity of the cell can be lumped into single parameter.

Figure 3 shows the word bond graph for the AEM cell including the membrane electrode assembly (MEA), electrolyte supply tank, gas separators and the power source. Word bond graph represents the components of the system and the nature of power exchange between them. It can be seen that this power exchange in the system belongs to multiple physical domains such as electro-chemical, thermal, thermo-fluidic. The coupling between different domains make the modelling even more challenging. Fig 4 shows the bond graph for the considered system. Each phenomenon considered will be discussed one by one. The electro-chemical phenomenon is considered instantaneous and is responsible for the overall cell voltage. It is represented through an algebraic equation given by the 1_{ec} and 1_{ov} junctions.

$$E_{cell} = E_{rev} + E_{ohm} + E_{act,cat} + E_{act,ano} \tag{4}$$

where E_{cell} represents the overall cell voltage, E_{rev} reversible potential, E_{ohm} is ohmic overvoltage, $E_{act,cat}$ and $E_{act,ano}$ are activation overvoltages. The transformer element TF_{ec} represents the conversion of electricity into chemical energy which is expressed by the equations (5) and (6) [6].

$$\dot{\zeta} = \frac{I_{cell}}{2F} \tag{5}$$

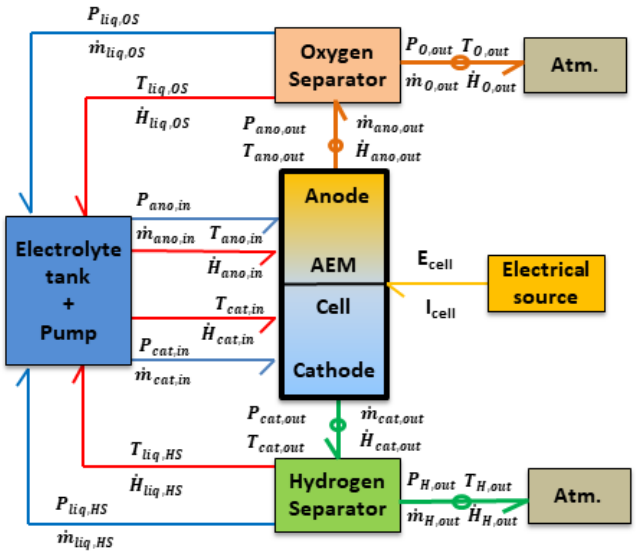

Fig. 3. Word bond graph for AEM cell

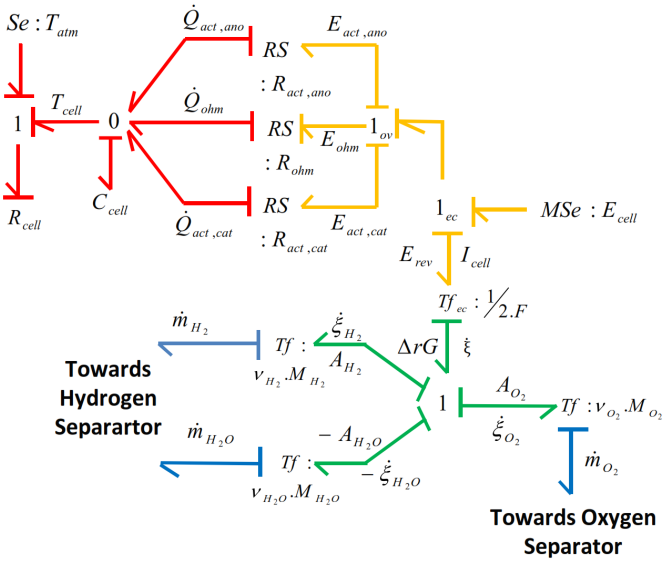

Fig. 4. Bond graph for AEM cell

$$E_{rev} = \frac{\Delta G}{2F} \tag{6}$$

The reversible potential is the minimum voltage to be applied along the cell in order to start the electrolysis. The value of it depends on temperature, molar concentration and vapour pressure of the KOH solution[15] and can be expressed by the equation (7)

$$E_{rev} = E^{o}_{rev,T} + \frac{R(T+273.5)}{2F} ln\left(\frac{(P-P_{v,KOH})\sqrt{(P-P_{v,KOH})}}{a_{H_2O,KOH}}\right) \tag{7}$$

Here, the R is the ideal gas constant,F is the Faraday's constant, T is the temperature in ^{o}C, P is the operating pressure (in bar), $P_{v,KOH}$ is the vapour pressure of KOH and $a_{H_2O,KOH}$ is the water activity in the KOH solution. $E^{o}_{rev,T}$ is the reversible voltage as standard pressure (1bar). It is the function of temperature and is expressed as [15]

$$\begin{aligned} E^{o}_{rev,T} = {} & 1.5184 - 1.5421\times10^{-3}(T+273.5) + 9.526 \\ & \times10^{-5}(T+273.5)ln(T+273.5) + 9.84 \\ & \times10^{-8}(T+273.15)^2 \end{aligned} \tag{8}$$

Following equations are used to calculate vapour pressure of KOH solution[15]

$$P_{v,KOH} = exp(2.302\,a + b\,lnP_{v,H_2O}) \tag{9}$$

$$a = -0.0151m - 1.6788\times10^{-3}m^2 + 2.2588\times10^{-5}m^3 \tag{10}$$

$$b = 1 - 1.2062\times10^{-3}m + 5.6024\times10^{-4}m^2 - 7.8228\times10^{-6}m^3 \tag{11}$$

$$\begin{aligned} P_{v,H_2O} = {} & exp(81.6179 - \tfrac{7699.68}{T+273.15} - 10.9ln(T+273.5) \\ & +9.5891\times10^{-3}(T+273.5)) \end{aligned} \tag{12}$$

where, m is the molar concentration of the KOH.

The water activity of KOH solution is given by the following expression [15]

$$a_{H_2O,KOH} = \left(-0.05192m + 0.003302m^2 + \tfrac{(3.177m - 2.131m^2)}{(T+273.5)}\right) \tag{13}$$

The activation overvoltages appear due to the kinetics of charge transfer between the electrode and the electrolyte. It is expressed by the Butler-Volmer equation [6].

$$J_{cell} = J_k\left[exp\left(\frac{\alpha_k.z.F.E_{act,k}}{R.T}\right) - exp\left(-\frac{(1-\alpha_k).z.F.E_{act,k}}{R.T}\right)\right] \tag{14}$$

where, J_{cell} is the current density, J_k is the current exchange density of the half reaction occurring at the two electrodes,α_k is the charge transfer coefficient and $E_{act,k}$ are the activation overvoltages for both electrodes. This equation is further simplified by considering equal charge transfer coefficient for both cathode and anode equal to 0.5[6] which is true for low current densities usually less than $2Acm^2$. This equation can be rewritten for calculating activation overvoltages as [6]

$$E_{act,k} = \frac{R(T+273.15)}{F} sinh^{-1}\left(\frac{J_{cell}}{2J_k}\right) \tag{15}$$

These overvoltages are modelled as two non linear resistance elements (RS element) $R_{act,cat}$ and $R_{act,ano}$ which contributes towards increasing the temperature of the cell. The third RS element (R_{ohm} represents the ohmic resistance of the cell, the equation of which is written as [7]

$$R_{ohm} = \left(R_{contact} + \frac{L_M}{A_M\sigma_M}\right) \tag{16}$$

$$E_{ohm} = I.R_{ohm} \tag{17}$$

where, $R_{contact}$ is the resistance of the cell except membrane, L_M is the thickness, A_M is the area and σ_M is the ionic conductivity of the membrane. The value of σ_M (in $\Omega^{-1}m^{-1}$) depends on temperature and is given by the equation (18)

$$\sigma_M = 198.3exp\left(-\tfrac{11190}{R(T+273.15)}\right) \tag{18}$$

In order to determine the current exchange densities an the resistance of the cell, these parameters are needed to be estimated using curve fitting of the polarisation curve. Due

to lack of more experimental that at present such as Electrochemical Impedance Spectroscopy (EIS), it is not possible to identify the current exchange densities separately. Therefore it is assumed that the current exchange densities are equal for both half reactions so that we can see their overall effect on the polarisation curve. Also, these overvoltages act as the source of heat which tends to increase the temperature of the cell. To model this, lumped thermal capacity C_{cell} of the cell is considered. The equation for the cell temperature can be then written as

$$T_{cell} = \frac{1}{C_{cell}} \int \left(\dot{Q}_{act,ano} + \dot{Q}_{act,cat} + \dot{Q}_{ohm} - \frac{T_{cell} - T_{atm}}{R_{cell}} \right) .dt \tag{19}$$

where, $\dot{Q}_j$ are the heat flows due to different overvoltages, T_{atm} is the ambient temperature and R_{cell} is the thermal resistance of the cell. Mass flows of the species produced and consumed are represented through TF elements as shown in Fig. 4. The mass flows of the species are calculated as

$$\dot{m}_i = v_i.M_i.\dot{\zeta} = v_i.M_i \frac{I_{cell}}{2F} \tag{20}$$

where m_i represents mass flow of the species i, v_i and M_i are the stoichiometry coefficient and molar mass of the species i.

III. Parameters Identification and Model Validation

For validation and simulation, a MATLAB Simulink model has been deduced systematically from the graphical bond graph model. Parameters are identified by curve fitting the polarisation curve of an actual cell. The polarisation curve has been provided by University of Exeter for their newly developed AEM cell. The characteristics of this cell are shown in the table III

A. Parameters Identification

To achieve the curve fitting of the polarisation curve for the identification of the parameters, Levenberg-Marquardt algorithm has been used. The equation of the polarisation curve can be written as

$$E_{cell} = E^o_{rev,T} + \frac{R(T+273.5)}{2F} ln \left(\frac{(P - P_{v,KOH})\sqrt{(P - P_{v,KOH})}}{a_{H_2O,KOH}} \right) + \frac{2R(T+273.15)}{F} sinh^{-1} \left(\frac{J_{cell}}{2J_k} \right) + I. \left(R_{contact} + \frac{L_M}{\sigma_M} \right) \tag{21}$$

Here the fitting parameters are J_k and $R_{contact}$. After fitting the values of J_k and $R_{contact}$ are found to be 4.337×10^{-7} Acm^{-2} and 0.0518 Ω respectively.

TABLE III
Specifications of the AEM cell

Specification	Value
Thickness of the membrane	25-50 μm
Area of the membrane	9 cm^2
Operating Pressure	1 bar
Operating temperature range	20-80 ^{o}C
KOH Concentration	4M
Input and output flow rates	250 ml/min

B. Validation

Figure 5 shows the plot of the actual and simulated polarisation curve. The model simulates the polarisation curve satisfactorily as the mean absolute percentage error (MAPE) of the model over considered data is 0.31%.

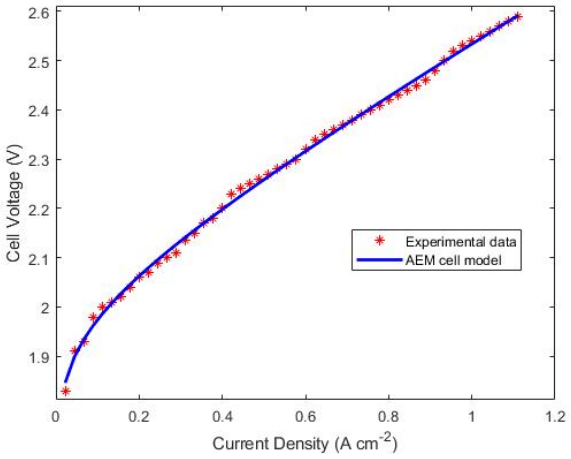

Fig. 5. Comparison of polarisation curve at 80 ^{o}C and 4M KOH

IV. Simulation and Discussion

Figure 6 shows the simulation of the polarisation curve for different temperatures and fixed concentration of 4M KOH. It can be seen that the voltage increases with increase in temperature. This phenomenon is probably due to the technology of membrane and need further experimental investigation for the confirmation. Simulation of the polarisation curve for

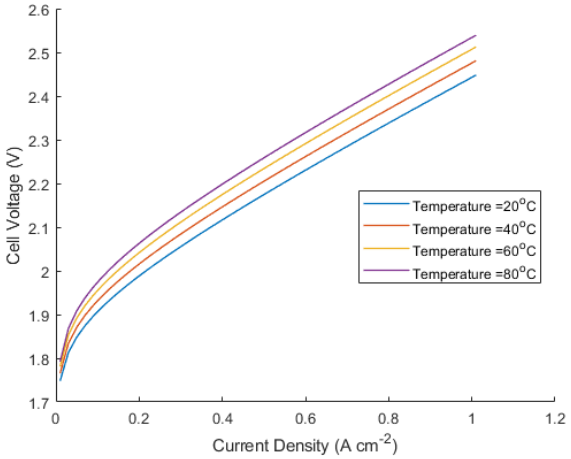

Fig. 6. Simulated polarisation curves for different temperatures at 4M KOH

fixed temperature of 80 ^{o}C and different concentrations of KOH is shown in the Fig.7. There is a negligible effect of the molar concentration on cell voltage as molar concentration appears in the equation of the reversible voltage only. Figure 8 shows the qualitative simulation of temperature evolution for the AEM cell. These simulations shows that different

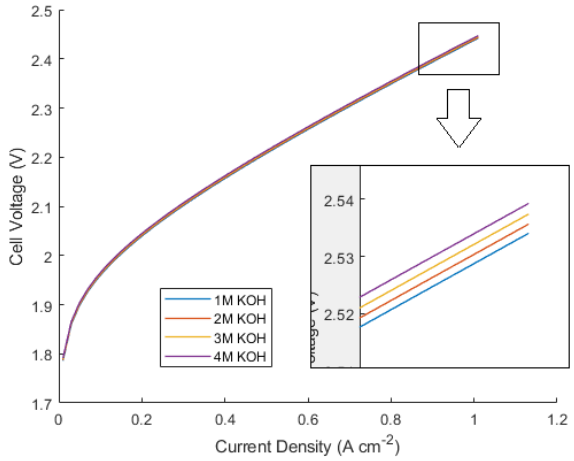

Fig. 7. Simulated polarisation curves for various conc. of KOH at 80^oC

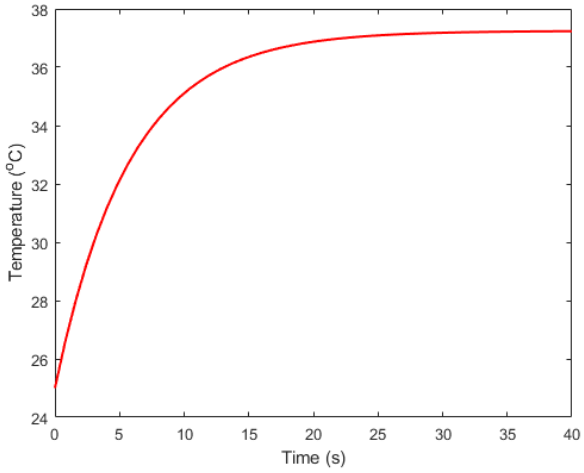

Fig. 8. Simulation of temperature evolution of the cell at constant current density of $0.5Acm^{-2}$

operating conditions can be tested virtually. This can help in decreasing the cost and the time involved due to experimental testing and could prove as a great tool for design optimization.

V. Conclusion

AEM water electrolysis is a developing technology that requires lots of research to be a matured like PEM water electrolysis so as to see its commercial application. In an attempt to contribute towards this technology a bond graph based multiphysics model for AEM cell has been developed. The developed model is then used to systematically generate MATLAB Simulink model which is used for the simulations of polarisation curve at different operating conditions. The results shows that the model can predict the polarisation curve satisfactorily. Further improvement in the model can be done by performing electrochemical impedance spectroscopy in order to identify current exchange densities for both anode and cathode separately. Also the model can be further enhanced by modelling the auxiliaries and other phenomenon like thermo-fluidic, mass transport etc. which can be then added into a single model. It will be really interesting to also test and validate the sizing of the model in order to see its implementation for AEM stack.

VI. Acknowledgment

S. Sood is a PhD. student at University of Lille. His work is funded under the E2C project funded by the Interreg 2 Seas-Program 2014-2020, co-financed by the European Fund for Regional Development in the frame of subsidiary contract nr. 2S03-019.

References

[1] I. P. Jain, "Hydrogen the fuel for 21st century," *International Journal of Hydrogen Energy*, vol. 34, no. 17, pp. 7368–7378, 2009.

[2] P. Olivier, C. Bourasseau, and B. Ould Bouamama, "Low-temperature electrolysis system modelling: A review," *Renewable and Sustainable Energy Reviews*, vol. 78, pp. 280–300, 2017.

[3] M. David, C. Ocampo-Martínez, and R. Sánchez-Peña, "Advances in alkaline water electrolyzers: a review," *Journal of Energy Storage*, vol. 23, pp. 392–403, 2019.

[4] I. Vincent and D. Bessarabov, "Low cost hydrogen production by anion exchange membrane electrolysis: A review," *Renewable and Sustainable Energy Reviews*, vol. 81, pp. 1690–1704, 2018.

[5] L. C. Seitz, T. J. Hersbach, D. Nordlund, and T. F. Jaramillo, "Enhancement effect of noble metals on manganese oxide for the oxygen evolution reaction," *The Journal of Physical Chemistry Letters*, vol. 6, no. 20, pp. 4178–4183, 2015.

[6] P. Olivier, C. Bourasseau, and B. Ould Bouamama, "Dynamic and multiphysic pem electrolysis system modelling: A bond graph approach," *International Journal of Hydrogen Energy*, vol. 42, no. 22, pp. 14 872–14 904, 2017.

[7] L. An, T. Zhao, Z. Chai, P. Tan, and L. Zeng, "Mathematical modeling of an anion-exchange membrane water electrolyzer for hydrogen production," *International Journal of Hydrogen Energy*, vol. 39, no. 35, pp. 19 869–19 876, 2014.

[8] I. Abdallah, "Event-driven hybrid bond graph: Application: hybrid renewable energy system for hydrogen production and storage," Ph.D. dissertation, Université de Lille, France, 2017.

[9] K. Onda, T. Murakami, T. Hikosaka, M. Kobayashi, and K. Ito, "Performance analysis of polymer-electrolyte water electrolysis cell at a small-unit test cell and performance prediction of large stacked cell," *Journal of The Electrochemical Society*, vol. 149, no. 8, pp. A1069–A1078, 2002.

[10] K. Agbli, M. Péra, D. Hissel, O. Rallières, C. Turpin, and I. Doumbia, "Multiphysics simulation of a pem electrolyser: Energetic macroscopic representation approach," *International Journal of Hydrogen Energy*, vol. 36, no. 2, pp. 1382–1398, 2011.

[11] T. Zhou and B. Francois, "Modeling and control design of hydrogen production process for an active hydrogen/wind hybrid power system," *International Journal of Hydrogen Energy*, vol. 34, no. 1, pp. 21–30, 2009.

[12] L. Xiao, S. Zhang, J. Pan, C. Yang, M. He, L. Zhuang, and J. Lu, "First implementation of alkaline polymer electrolyte water electrolysis working only with pure water," *Energy & Environmental Science*, vol. 5, no. 7, pp. 7869–7871, 2012.

[13] H. Ito, N. Miyazaki, S. Sugiyama, M. Ishida, Y. Nakamura, S. Iwasaki, Y. Hasegawa, and A. Nakano, "Investigations on electrode configurations for anion exchange membrane electrolysis," *Journal of Applied Electrochemistry*, vol. 48, no. 3, pp. 305–316, 2018.

[14] B. Ould Bouamama, I. Abdalah, and A.-L. Gehin, "Bond graphs as mechatronic approach for supervision design of multisource renewable energy system," in *IOP Conference Series: Materials Science and Engineering*, vol. 417, no. 1. IOP Publishing, 2018, p. 012033.

[15] A. Ursúa and P. Sanchis, "Static–dynamic modelling of the electrical behaviour of a commercial advanced alkaline water electrolyser," *International Journal of Hydrogen Energy*, vol. 37, no. 24, pp. 18 598–18 614, 2012.